Supporting information

Contents

1. Materials and methods

All chemicals were purchased from commercial suppliers and used as received unless otherwise specified. Column chromatography was carried out with silica gel for flash chromatography from VWR Scientific. ^{1}H and ^{13}C NMR spectra were recorded on a Bruker Model 400 spectrometer. UV−vis absorption spectra were recorded on a UV-1601 Shimadzu UV−vis spectrometer. DSC experiments were carried out with a Netzsch DSC-204 F1 instrument at a heating rate of 10 °C/min under nitrogen. Thermal Gravimetric Analysis (TGA) was carried out on a Thermogravimetric Analyzer from Nicolet 6700 at a rate of 10 °C/min under nitrogen. Single crystal data collection was carried out on an agilent X-Ray single crystal diffractometer. Emission spectra were recorded on a fluorescence spectrometer from Hitachi F-6000. Cyclic voltammetry (CV) was performed using an Autolab PGSTAT101 potentiostat with a standard three-electrode system consisting of a cylindrical platinum working electrode, platinum mesh counter electrode and Ag/Ag^{+} reference electrode, calibrated against ferrocene. Measurements were carried out on the acceptors (3×10^{-4} M) in anhydrous and deoxygenated dichloromethane with 0.1 M of tetrabutylammonium hexafluorophosphate ($TBAPF_6$) as the supporting electrolyte.

OFET devices for AIID-12, FAIID-12 and AIID-14 were fabricated in a BGBC configuration. A layer of 300 nm thick SiO_2 was used as a gate dielectric layer and a heavily doped n-type silicon wafer was chosen as the gate electrode. Thin films of AIID-12, FAIID-12 and AIID-14 were spin-coated from 8 mg. mL-1 hexane and chloroform (V/V=1:3) solution. The gold drain/source (D/S) electrodes were adopted and deposited on the substrates by photo-lithography. All devices were measured in

glove box with Bottom-Gate Bottom-Contact (BGBC) configuration (Gold strips). Electrical characteristics of the devices were recorded with a Keithley 4200-SCS semiconductor parameter analyzer and a Micromanipulator 6150 probe station in a glove box at room temperature. X-ray diffraction (XRD) measurement was performed in reflection mode at 40 kV and 200 mA with Cu Ka radiation using a 2 kW Rigaku D/max-2500 X-ray diffractometer. AFM was measured on a Cyhper Es.

2. Absorption spectra

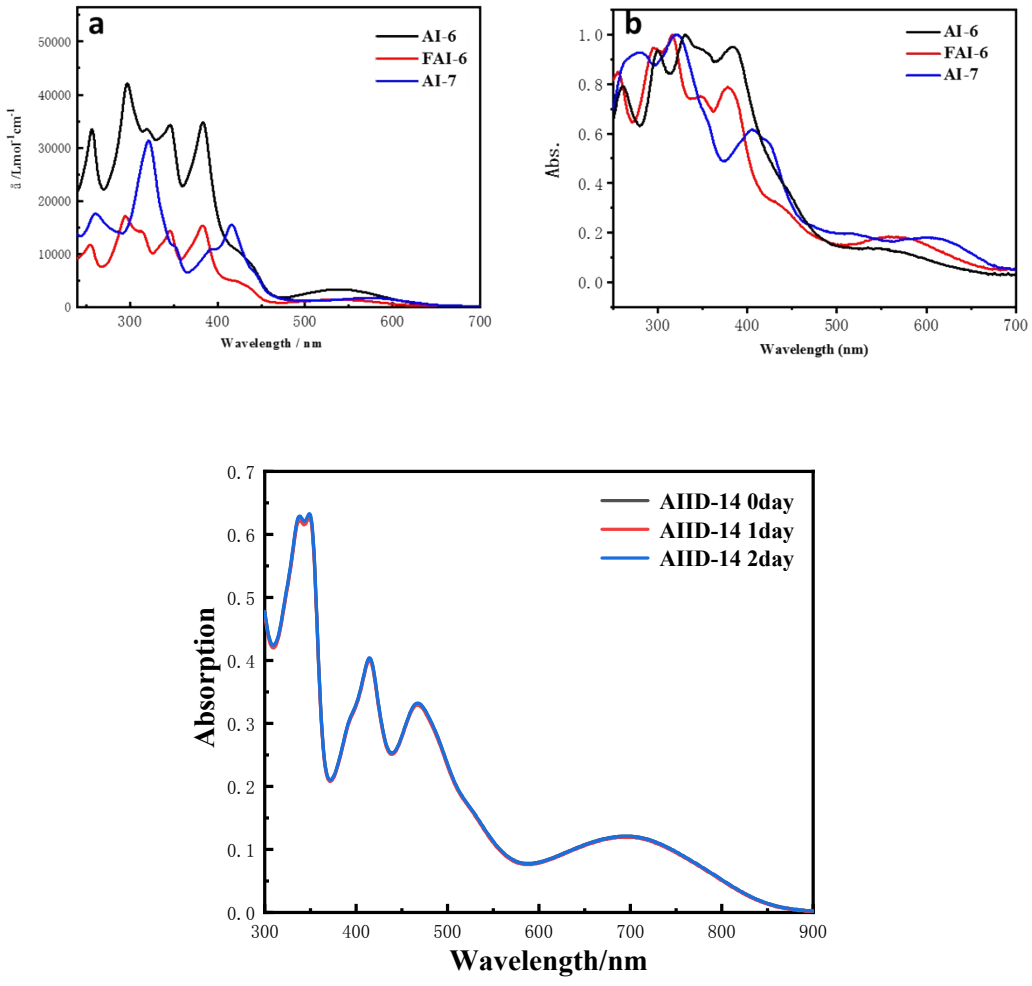

Figure S1: The absorption spectra of AI-6, FAI-6 and AI-7 in $CHCl_3$ solution (a), in thin films (b) and AIID-14 in $CHCl_3$ solution after 2 days.

3. CVs of compounds

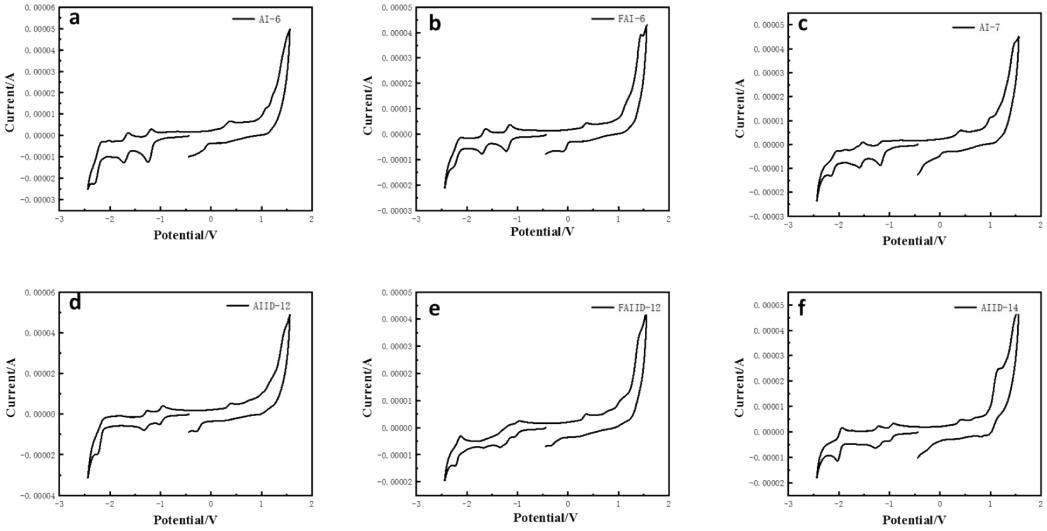

Figure S2: The CV curves of AI-6, FAI-6, AI-7, IID, AIID-12, FAIID-12 and AIID-14.

4. TGA of compounds

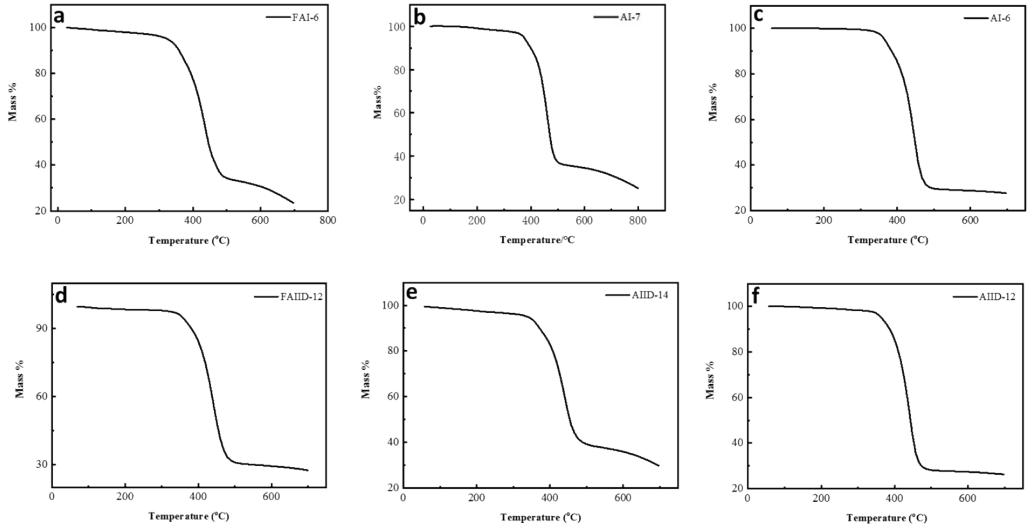

Figure S3: The TGA data of compounds. (360 °C for AI-6, 320 °C for FAI-6, 372 °C for AI-7, 365 °C for AIID-12, 360 °C for FAIID-12, 338 °C for AIID-14).

5. DSC of compounds

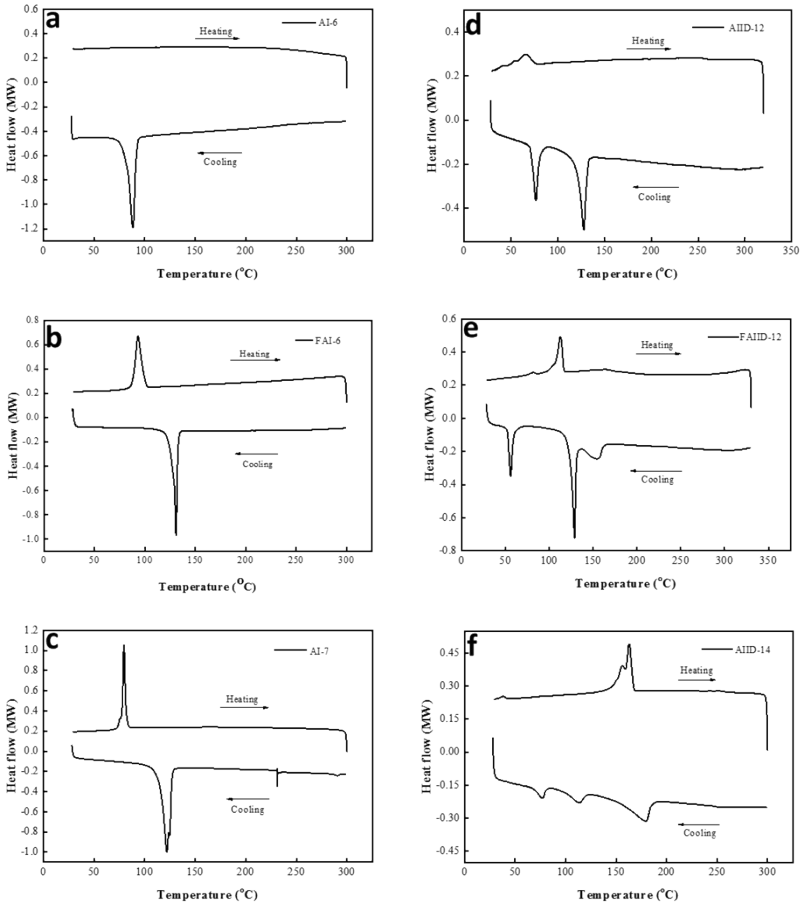

Figure S4: DSC data of AI-6, FAI-6, AI-7, AIID-12, FAIID-12 and AIID-14.

6. DFT calculations:

Geometry optimization of all molecules considered in this study were carried out at the B3LYP/6-31G(d,p) level of theory. The alkyl side-chains substituted on the backbone were replaced with methyl groups to reduce the computational cost. Vertical excitation energies were calculated using TDDFT methodology based on the ground state geometries. All calculations were performed with the Gaussian16 software. [1]

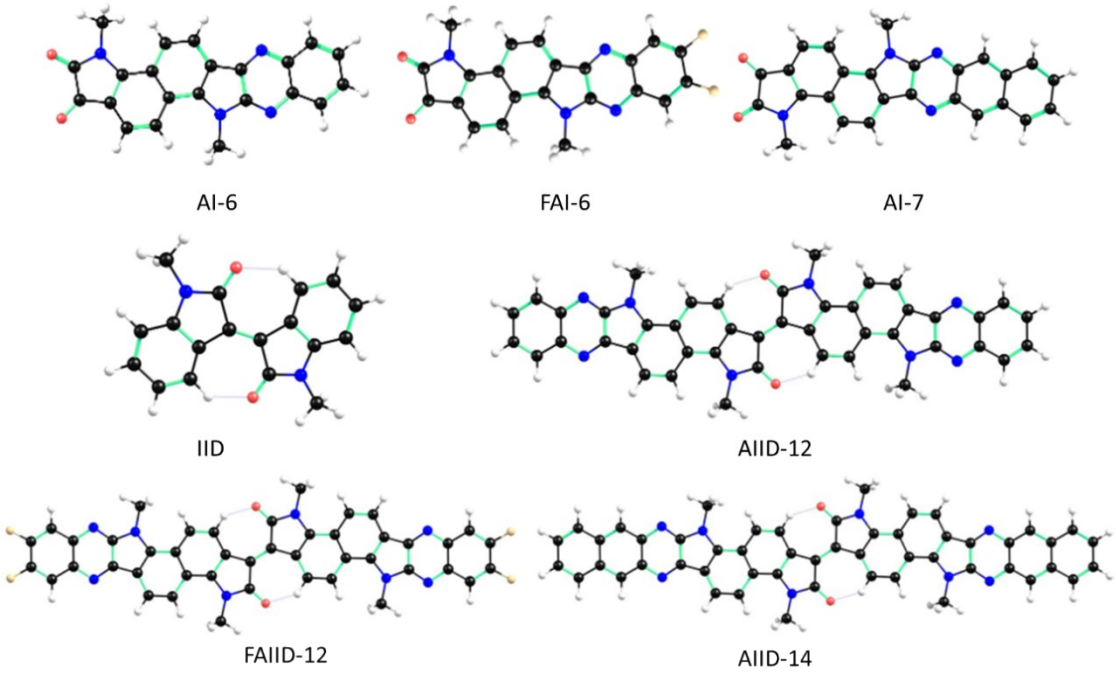

Figure. S5 Optimized geometries of molecules AI-6, FAI-6, AI-7, IID, AIID-12, FAIID-12 and AIID-14 calculated at B3LYP/6-31G(d,p) level of theory

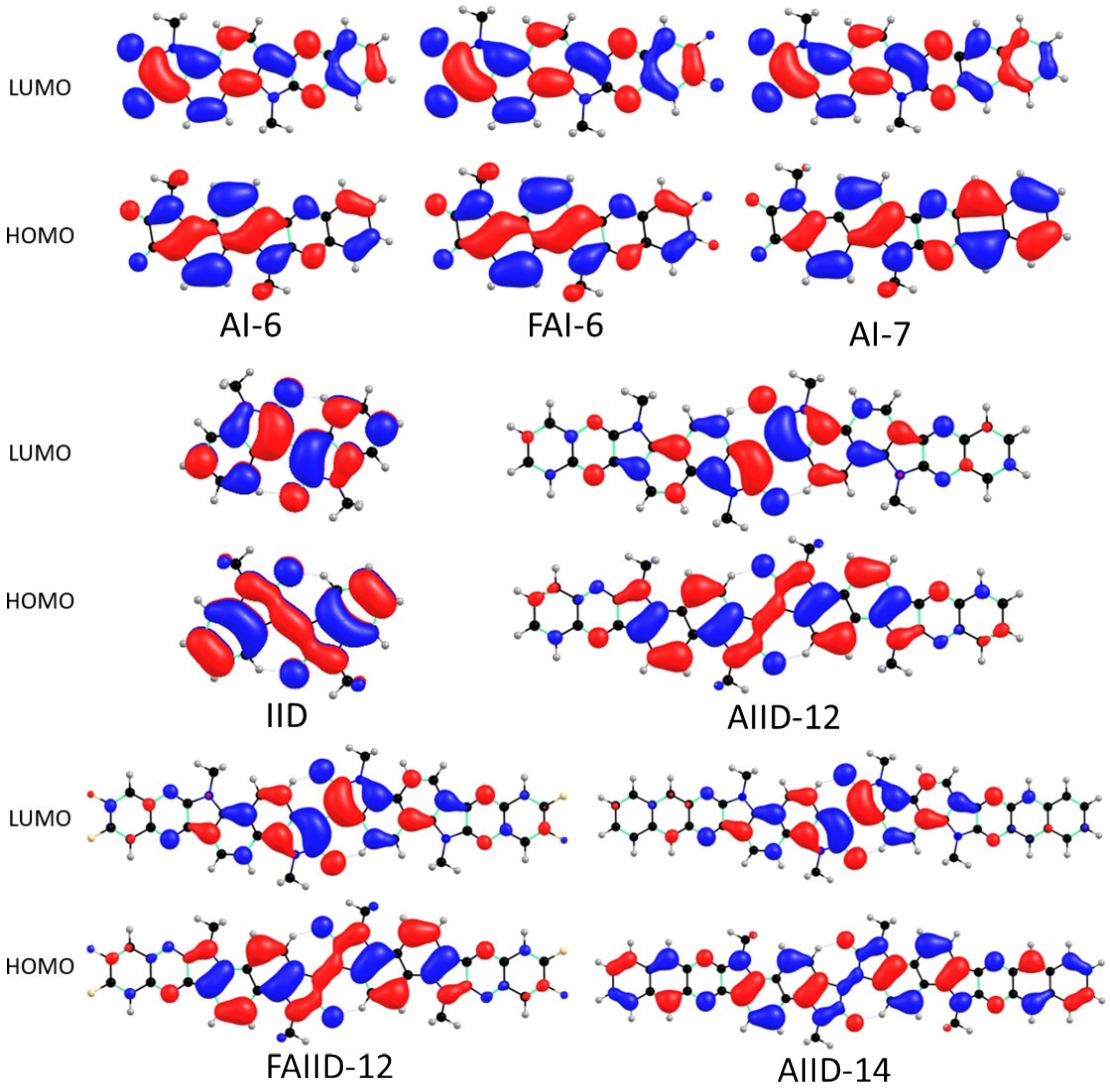

Figure S6: HOMO-LUMO wavefunctions of molecules AI-6, FAI-6, AI-7, IID, AIID-12, FAIID-12 and AIID-14 calculated at B3LYP/6-31G(d,p) level of theory.

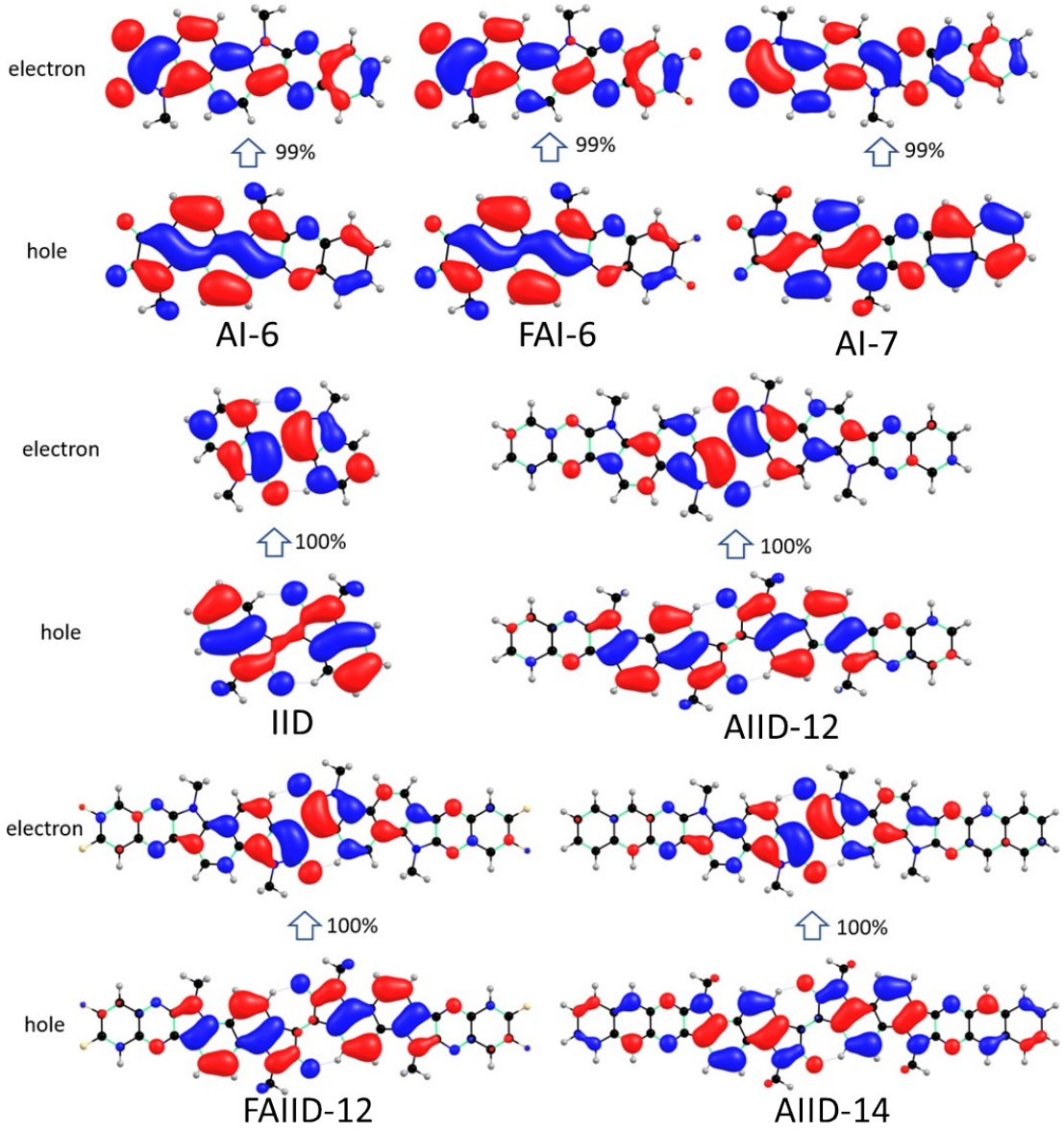

Figure S7: The natural transition orbitals (NTO) describing the $S_0 \rightarrow S_1$ transition of **AI-6**, **FAI-6**, **AI-7**, Y, AIID-12, FAIID-12 and AIID-14 at B3LYP/6-31G(d,p) level of theory

Table-S1: HOMO-LUMO energies (eV) and reorganization energies (meV) of AI-6, FAI-6, AI-7, IID, AIID-12, FAIID-12 and AIID-14.

Comp.	HOMO	LUMO	HOMO-LUMO (eV)	reorg hole (meV)	reorg electron(meV)
AI-6	-5.65	-2.88	2.77	250	250
FAI-6	-5.78	-3.00	2.79	280	250
AI-7	-5.43	-2.96	2.47	120	210
AIID-12	-5.16	-3.10	2.06	180	300
FAIID-12	-5.31	-3.24	2.08	200	300
AIID-14	-5.07	-3.16	1.91	80	240
IID	-5.60	-2.64	2.95	250	450

7. Device data

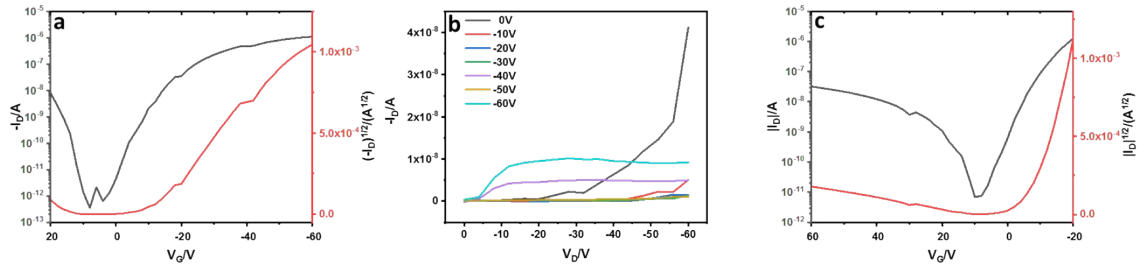

Figure S8: Pristine films of **AIID-12** with W/L = 1400/10.

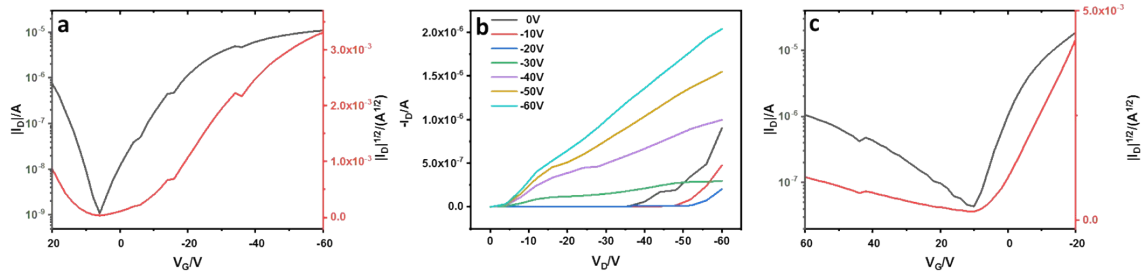

Figure S9: Spin coating films under thermal annealing at 60 °C of AIID-12 with W/L = 1400/10.

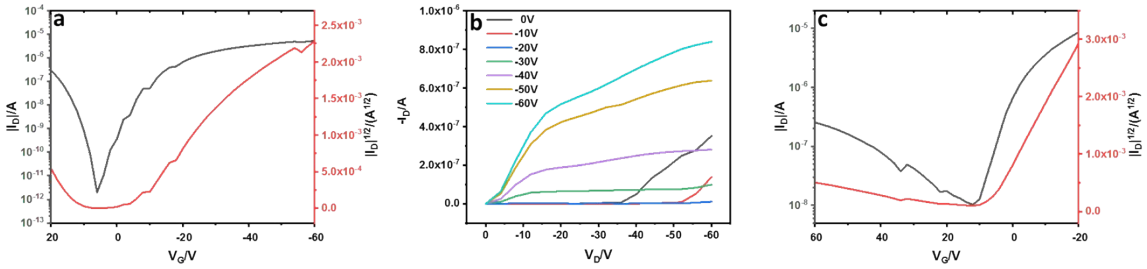

Figure S10: Spin coating films under thermal annealing at 60 °C of AIID-12 with W/L = 1400/20.

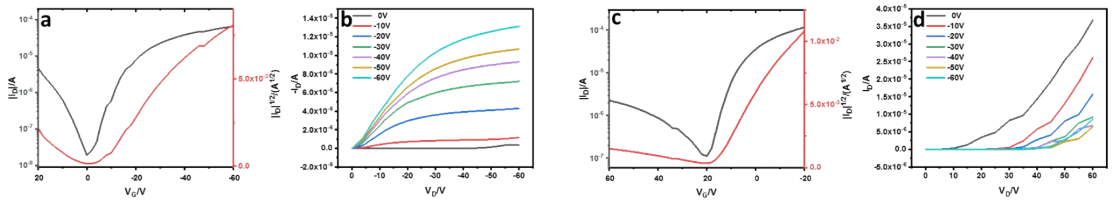

Figure S11: Pristine films of output curves of AIID-14 with W/L = 1400/10.

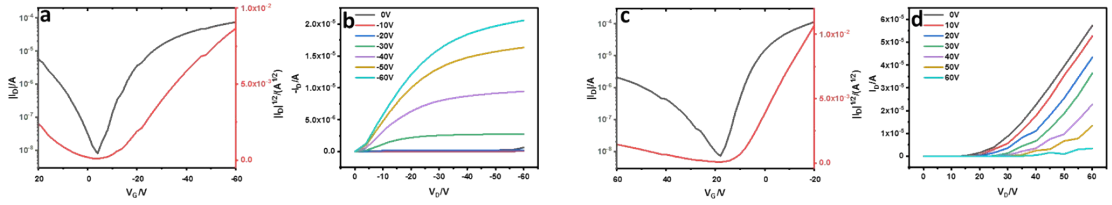

Figure S12: Spin coating films under thermal annealing at 60 °C of output curves of AIID-14 with W/L = 1400/10.

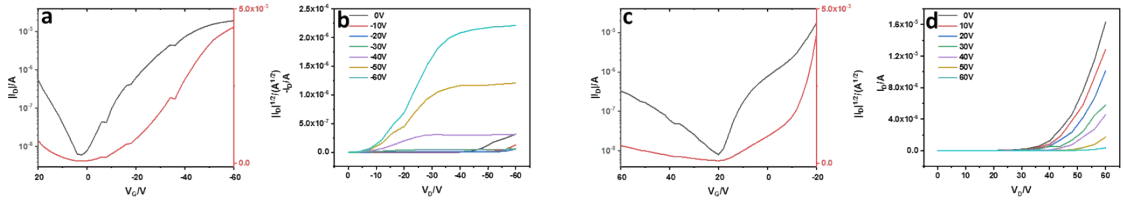

Figure S13: Spin coating films under thermal annealing at 120 °C of output curves of AIID-14 with W/L = 1400/10.

Table S2: Summarize of the mobilities of AIID-12 based devices

	Pristine films		60°C annealing	
W/L	Mobilities [$cm^2 V^{-1}s^{-1}$]	V_T [V]	Mobilities [$cm^2 V^{-1}s^{-1}$]	V_T [V]
1400/10	h=1.4×10^{-3}	-20.0	h=1.2×10^{-2}	-8.54
	e= 4.4×10^{-5}	19.0	e=8.6×10^{-4}	16.9
1400/20	h=2.2×10^{-3}	-15.0	h=1.0×10^{-2}	-6.60
	e= 3.2×10^{-5}	23.0	e=6.0×10^{-4}	20.6

Table S3: Summarize of the mobilities of AIID-14 based devices

	Pristine film		60°C annealing		120°C annealing	
W/L	Mobilities [$cm^2 V^{-1}s^{-1}$]	V_T [V]	Mobilities [$cm^2 V^{-1}s^{-1}$]	V_T [V]	Mobilities [$cm^2 V^{-1}s^{-1}$]	V_T [V]
1400/10	h=6.9×10^{-2}	-7.39	h=7.6×10^{-2}	-12.9	h=3.0×10^{-2}	-21.7
	e= 2.1×10^{-3}	16.7	e=2.9×10^{-3}	26.7	e=5.4×10^{-4}	30.2
1400/20	h=8.3×10^{-2}	-7.36	h=8.65×10^{-2}	-10.2	h=5.32×10^{-2}	-20.5
	e=5.4×10^{-4}	1.61	e=1.87×10^{-3}	13.9	e=3.44×10^{-4}	36.8

8. AFM

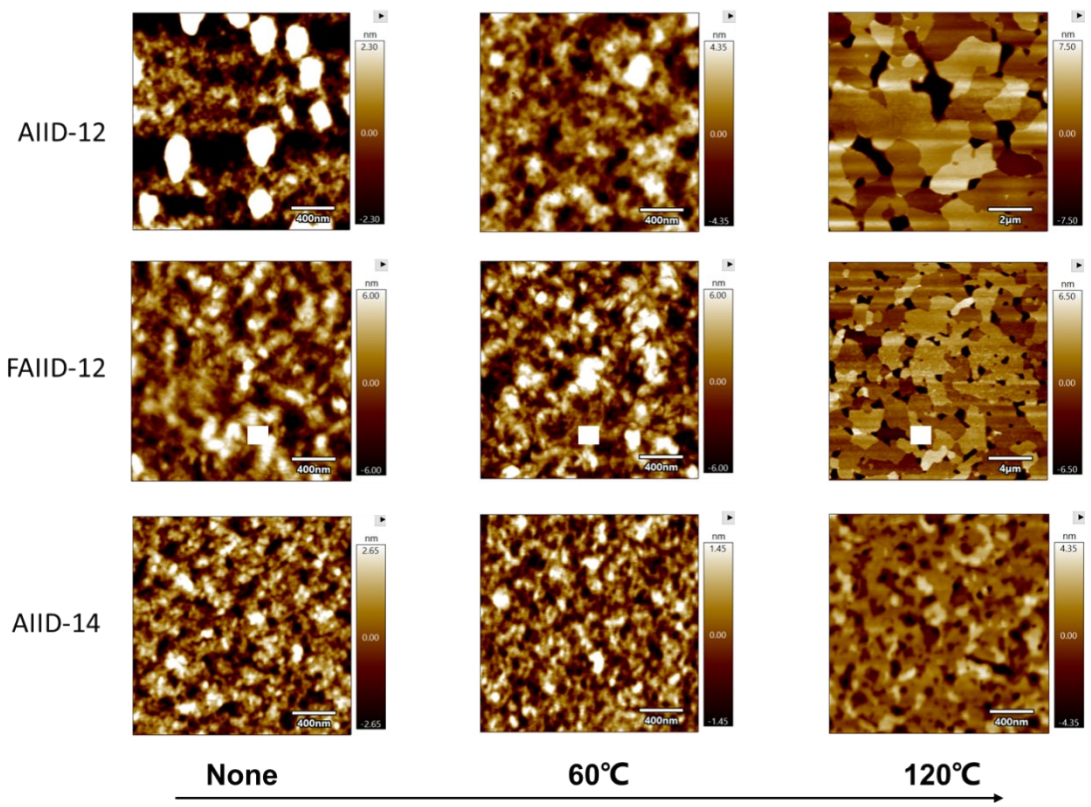

Figure S14: AFM images of Spin coating films of AIID-12, FAIID-12 and AIID-14 with none, 60 ºC and 120 ºC thermal annealing.

9. XRD

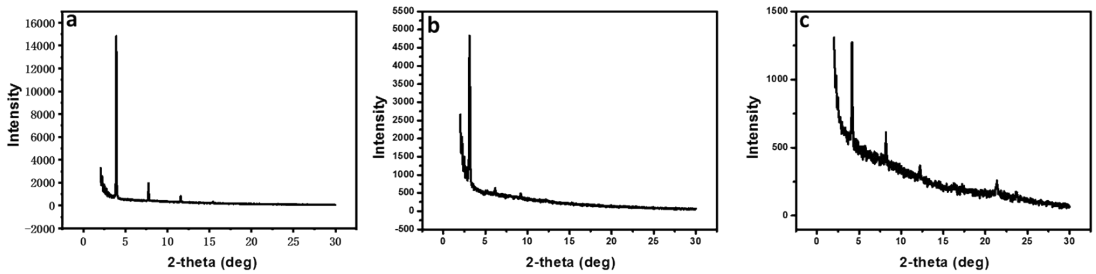

Figure S15: XRD data of Pristine films of AIID-12, FAIID-12 and AIID-14 without thermal annealing.

10. Synthesis and characterization

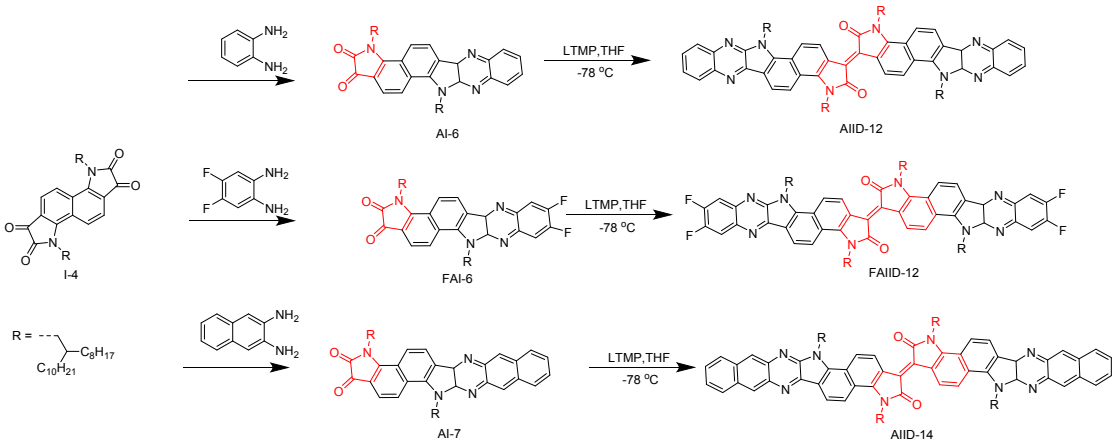

Scheme S1: An alternative synthesis route of aza-IID dimers according to literature procedure [2].

AI-6.

Benzene-1,2-diamine (10.90 mg, 0.10 mmol), 3,8-Bis-(2-octyl-dodecyl)-3,8-dihydro-indolo[7,6-e]indole-1,2,6,7-tetraone (50 mg,0.06 mmol) in acetic acid (5 mL) and chloroform (8 ml) was heated to 75 °C for 2 h under argon. The crude product was subjected to column chromatography using methylbenzene as eluting to get a brown solid (yield: 75 mg, 82.55 %). ^{1}H NMR (400 MHz, chloroform-d, 300 K), δ (ppm): 8.44 (d, *J* = 12 Hz,1H), 8.28 (d, *J* = 8.0 Hz, 1H), 8.18 (d, *J* = 8.0 Hz, 1H), 8.14 (d, *J* = 8.0 Hz, 1H), 8.02 (d, *J* = 8.0 Hz, 1H), 7.80 (t, 1H), 7.75 (t, 1H), 7.64 (d, *J* =8.0 Hz, 1H), 7.28 (s, 1H), 4.90 (d, *J* =8.0 Hz, 2H), 4.17 (d, *J* =8.0 Hz, 2H), 1.12-1.45 (m, 59H), 0.84-0.90 (m, 17H).

^{13}C NMR (100 MHz, $CDCl_3$, 300 K), δ (ppm):182.72, 160.11, 152.24, 146.23, 141.01, 140.69, 140.15, 136.95, 129.50, 129.15, 129.02, 128.50, 128.36, 128.21, 127.23, 125.28, 122.45, 120.00, 119.23, 119.02, 118.97, 117.09, 114.52, 77.33, 77.22, 77.02, 76.70, 48.30, 47.52, 37.83, 37.73, 31.91, 31.89, 31.87, 30.05, 29.62, 29.54, 29.52, 29.34, 29.29, 29.28, 22.66, 14.10, 14.07.

MS (MALDI-TOF, $CHCl_3$): Calculated for $C_{60}H_{92}N_4O_2$, 900.72, found: 900.0.

FAI-6.

4,5-Difluoro-benzene-1,2-diamine (4.36 mg, 0.03 mmol), 3,8-Bis-(2-octyl-dodecyl)-3,8-dihydro-indolo[7,6-e]indole-1,2,6,7-tetraone (30 mg, 0.04 mmol) in acetic acid (4 mL) and chloroform (10 ml) was heated to 75 °C for 1 h under argon. The crude product was subjected to column

chromatography using methylbenzene as eluting to afford a brown solid (yield: 20.5 mg, 72.29 %). ^{1}H NMR (400 MHz, chloroform-d, 300 K), δ (ppm): 8.58（d, *J* =12.0 Hz, 2H), 8.40 (d, *J* = 12.0 Hz, 2H), 8.25 (d, *J* = 12.0 Hz, 2H), 8.12 (d, *J* =12.0 Hz, 2H), 7.96 (m, 2H), 7.82 (d, *J* = 8.0 Hz, 2H), 5.02 (d, *J* = 8.0 Hz, 4H), 4.30 (d, *J* = 8.0 Hz, 4H),1.15-1.59 (m, 43H), 0.86 -0.90 (m, 33H).

^{13}C NMR (100 MHz, $CDCl_3$, 300 K), δ (ppm): 145.82, 141.32, 138.23, 137.95, 132.99, 130.69, 129.12, 128.24, 123.15, 118.65, 116.62, 116.17, 77.32, 77.21, 77.01, 76.69, 48.13, 38.02, 31.91, 31.85, 30.04, 29.68, 29.66, 29.62, 29.59, 29.34, 29.32, 22.68, 22.63, 14.11, 14.09.

MS (MALDI-TOF, $CHCl_3$): Calculated for $C_{60}H_{90}F_2N_4O_2$, 936.70, found: 936.0.

AI-7.

Naphthalene-2,3-diamine (3.16 mg, 0.02 mmol), 3,8-Bis-(2-octyl-dodecyl)-3,8-dihydro-indolo[7,6-e]indole-1,2,6,7-tetraone (20 mg,0.02 mmol) in acetic acid(2.5 mL) and chloroform (5 ml) was heated to 75 °C for 1.5 h under argon. The crude product was subjected to column chromatography using methylbenzene as eluting to afford a brown solid (yield: 15.1 mg,79.45 %). ^{1}H NMR (400 MHz, chloroform-d, 300 K), δ (ppm): 8.82（s, 2H), 8.63 (s, 2H), 8.44 (d, *J* = 8.0 Hz, 2H), 8.24 (d, *J* = 8.0 Hz, 2H), 8.12(d, *J* = 8.0 Hz, 2H), 8.08 (d, *J* = 8.0 Hz, 2H),8.01 (d, *J* =12 Hz, 2H),7.68 (d , *J* = 8.0 Hz, 2H), 7.59 (d, *J* = 8.0 Hz, 2H), 7.54 (d, *J* = 8.0 Hz, 2H), 4.93 (d, *J*=8.0 Hz, 4H), 4.16 (d, *J*=8.0 Hz, 4H), 1.04-1.45 (m, 46H), 0.80-0.90 (m, 30H).

^{13}C NMR (100 MHz, $CDCl_3$, 300 K), δ (ppm):211.31, 182.47, 160.03, 157.87, 152.13, 146.73, 142.13, 137.76, 131.88, 127.51, 126.39, 125.45, 123.16, 119,62, 119.27, 117.44, 114.42, 77.33, 77.21, 77.01, 76.69, 48.35, 48.09, 37.86, 31.91, 30.04, 29.90, 29.62, 29.55, 29.35, 22.68, 14.10, 14.03, 0.30.

MS (MALDI-TOF, $CHCl_3$): Calculated for $C_{64}H_{94}N_4O_2$, 950.74, found: 950.0.

AIID-12.

At-78 degrees Celsius and nitrogen, hexaethyltriaminophosphine was added to the mixed solution of **AI-6** (50 mg, 0.05 mmol) and dichloromethane (10 ml), and then stirred at room temperature for the overnight. The crude product was subjected to column chromatography using methylbenzene as eluting to give a brown solid (yield: 43 mg, 43.9 %). ^{1}H NMR (400 MHz, chloroform-d, 300 K), δ (ppm): 9.15 (d, J= 8Hz, 2H), 8.44 (d, *J*= 8.0 Hz, 2H), 8.32 (d, *J*= 8.0 Hz,

2H), 8,17 (d, *J*= 8.0Hz, 2H), 8.13 (d, *J*= 8.0 Hz, 2H), 8.07 (d, *J*= 8.0Hz, 2H), 7.61 (d, *J*= 8.0 Hz, 2H), 7.59 (d, *J*= 8.0 Hz, 2H), 4.96 (d, *J*= 8.0Hz, 2H), 4.40 (d, *J*= 8.0 Hz, 2H), 1.15-1.43 (m, 35H), 0.79-0.87 (m, 41H).

^{13}C NMR (100 MHz, $CDCl_3$, 300 K), δ (ppm):169.59, 146.04, 143.41, 140.84, 140.80, 140.15, 131.65, 129.03, 127.96, 125.31, 124.21, 121.80, 120.06, 118.32, 117.04, 77.32, 77.00, 76.68, 48.09, 46.95, 31.90, 31.87, 31.53, 30.90, 30.05, 29.64, 29.34, 29.27, 26.53, 25.99, 22.65, 14.10, 14.06.

MS (MALDI-TOF, $CHCl_3$): Calculated for $C_{120}H_{182}N_8O_2$, 1765.42, found: 1765.0.

Anal. Calcd for $C_{120}H_{182}N_8O_2$: C, 81.63; H, 10.42; N, 6.35. Found: C,81.88; H, 10.59; N, 5.83.

FAIID-12.

At -78 degrees Celsius and nitrogen, hexaethyltriaminophosphine was added to the mixed solution of **FAI-6** (50 mg, 0.05 mmol) and dichloromethane (10 ml), and then stirred at room temperature for the overnight. The crude product was subjected to column chromatography using methylbenzene as eluting to give a brown solid (29.8 mg, 29.6 % yield). ^{1}H NMR (400 MHz, chloroform-d, 300 K), δ (ppm): 9.14 (d, *J* = 8.0 Hz, 2H), 8.32 (d, *J* = 8.0 Hz, 2H), 8.12 (d, *J* = 8.0 Hz, 2H), 8.03 (dd, 4H), 7.70 (m, 2H), 4.86 (s, 4H), 4.39 (s, 4H), 1.18-1.45 (m, 47H), 0.90-0.92 (m, 29 H).

^{13}C NMR (100 MHz, $CDCl_3$, 300 K), δ (ppm):169.49, 150.54, 145.62, 143.31, 140.48, 137.38, 136.71, 131.91, 124.82, 121.39, 119.89, 118.10, 117.11, 116.46, 116.21, 114.28, 114.14, 113.17, 113.03, 77.27, 77.68, 76.77, 48.12, 47.43, 37.97, 37.68, 31.88, 30.09, 29.71, 29.65, 29.57, 27.36, 26.54, 25.94, 14.10, 14.07, 1.03, 0.00.

MS (MALDI-TOF, $CHCl_3$): Calculated for $C_{120}H_{178}F_4N_8O_2$, 1885.48, found: 1885.0.

Anal. Calcd for $C_{120}H_{178}F_4N_8O_2$: C, 76.44; H, 9.52; N, 5.94. Found: C, 77.16; H, 9.62; N, 5.20.

AIID-14.

At -78 degrees Celsius and nitrogen, hexaethyltriaminophosphine was added to the mixed solution of **AI-7** (50 mg, 0.05 mmol) and dichloromethane (10 ml), and then stirred at room temperature overnight. The crude product was subjected to column chromatography using methylbenzene as eluting to give a brown solid (yield: 17.8 mg, 18.19 %). ^{1}H NMR (400 MHz, chloroform-d, 300 K), δ (ppm): 9.09 (d, *J* = 8.0Hz, 2H), 8.46 (s, 2H), 8.28 (s, 2H), 8.17 (d, *J* = 8.0 Hz, 2H), 8.07 (d, *J* = 8.0 Hz, 2H), 7.95 (d, *J* = 8.0 Hz, 2H), 7.91 (d, *J* = 8.0 Hz, 2H), 7.70 (d, *J* = 8.0 Hz, 2H), 7.21 (m,

2H), 7.11(m, 2H), 4.84 (s, 4H), 4.41 (s, 4H), 2.38-1.04 (m, 63H), 0.92-0.18 (m, 63H).

^{13}C NMR (100 MHz, CDCl3, 300 K), δ (ppm):146.48, 143.29, 142.21, 139.79, 137.54, 137.44, 132.84, 131.70, 131.36, 128.07, 127.30, 126.98, 125.54, 124.70, 124.61, 124.55, 121.78, 119.86, 118.31, 116.97, 116.68, 77.28, 77.00, 76.77, 47.97, 47.41, 38.07, 37.82, 31.91, 31.55, 30.90, 30.16, 29.68, 29.36, 26.60, 26.04, 22.67, 14.09, 0.00.

MS (MALDI-TOF, $CHCl_3$): Calculated for $C_{128}H_{186}N_8O_2$,1867.47, found:1867.0.

Anal. Calcd for $C_{128}H_{186}N_8O_2$: C, 82.32; H, 10.04; N, 6.00. Found: C, 81.96; H, 10.10; N, 5.45.

11. **NMR figures**

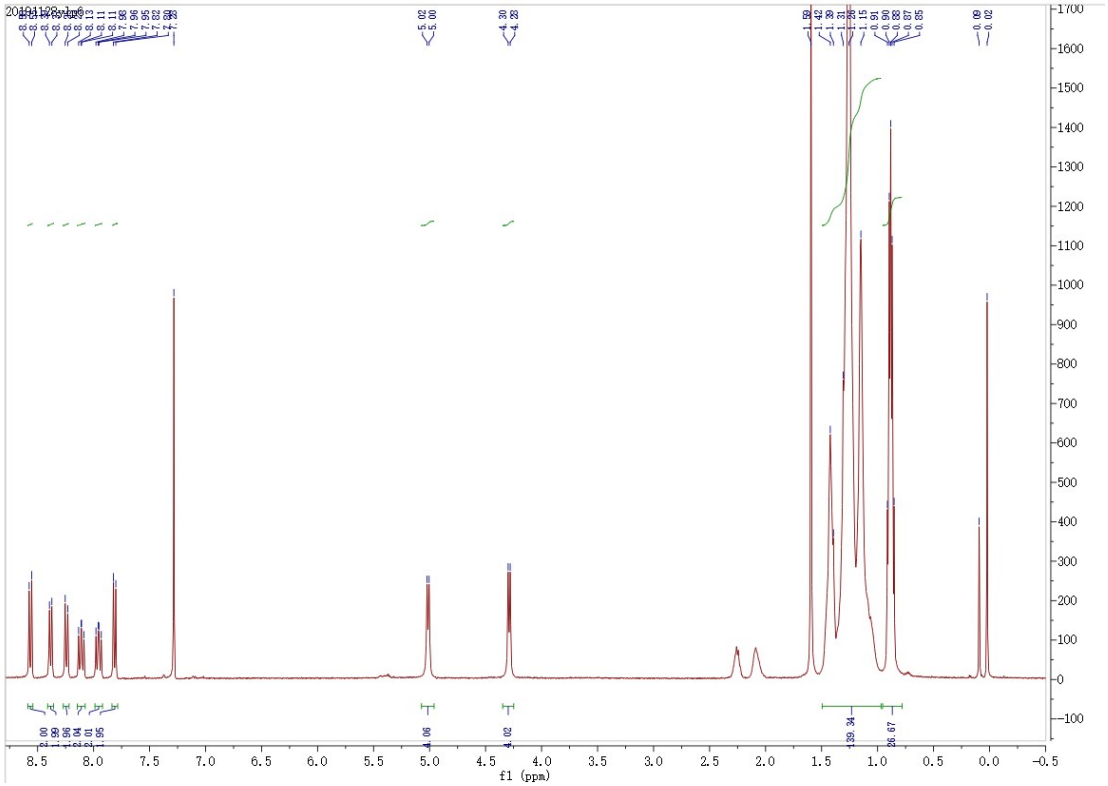

Figure S16:^{1}H NMR of **FAI-6** in $CDCl_3$ at 300K.

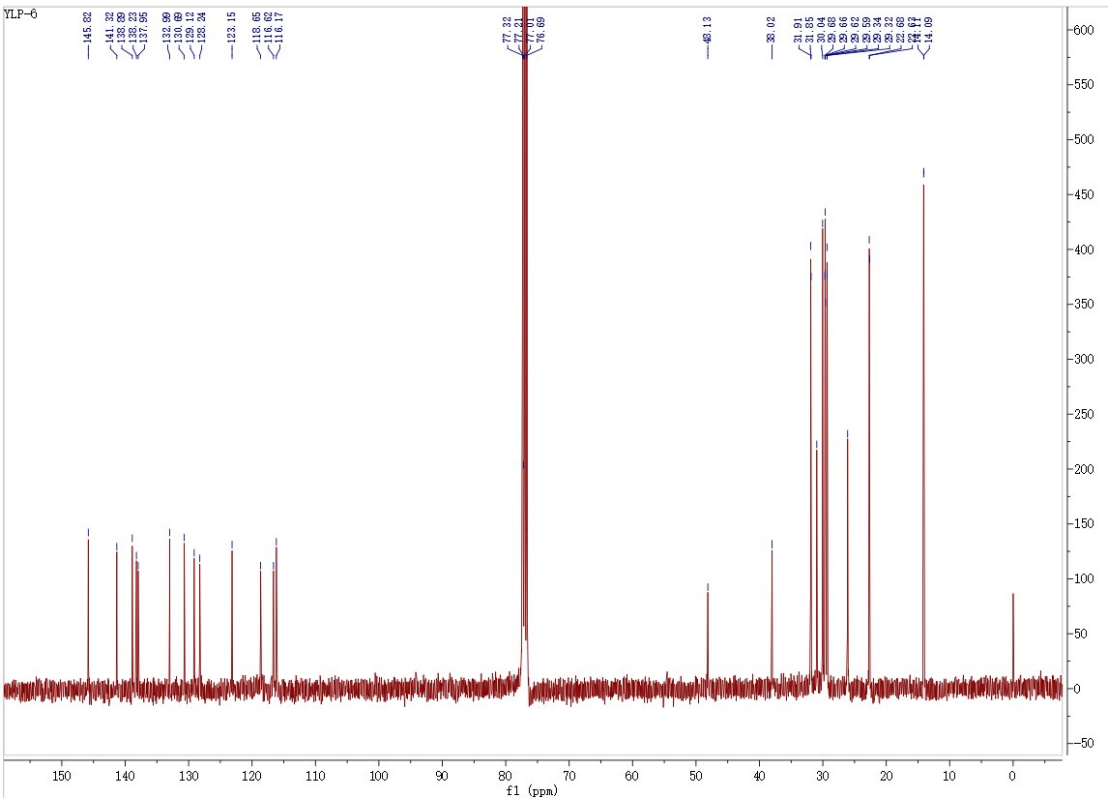

Figure S17:^{13}C NMR of **FAI-6** in $CDCl_3$ at 300K.

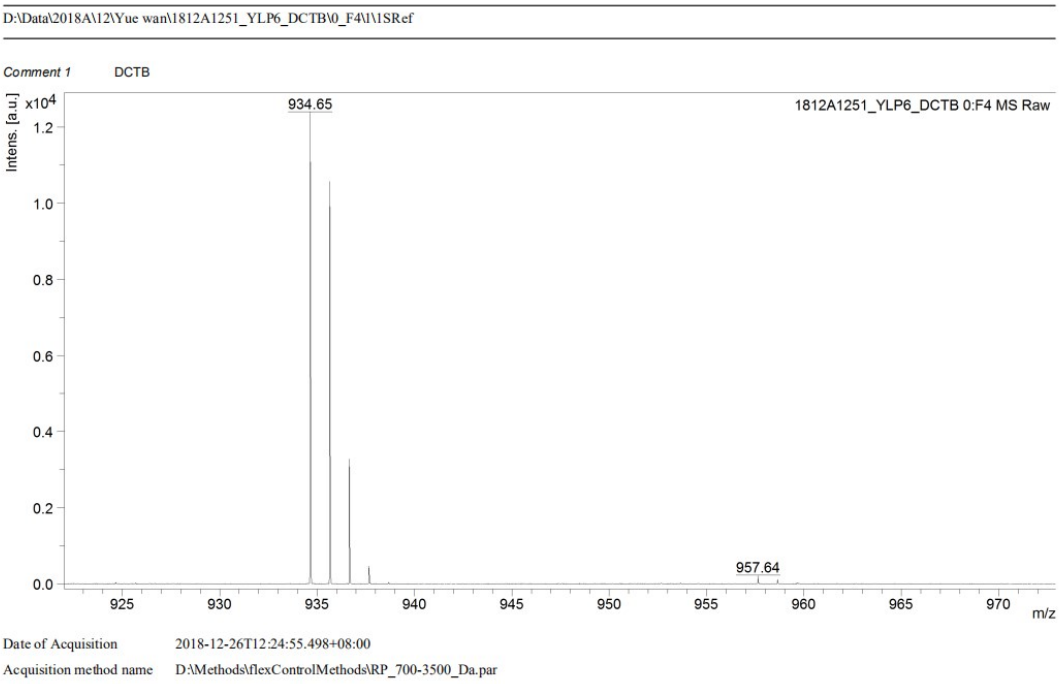

Figure S18: MALDI-TOF of **FAI-6**.

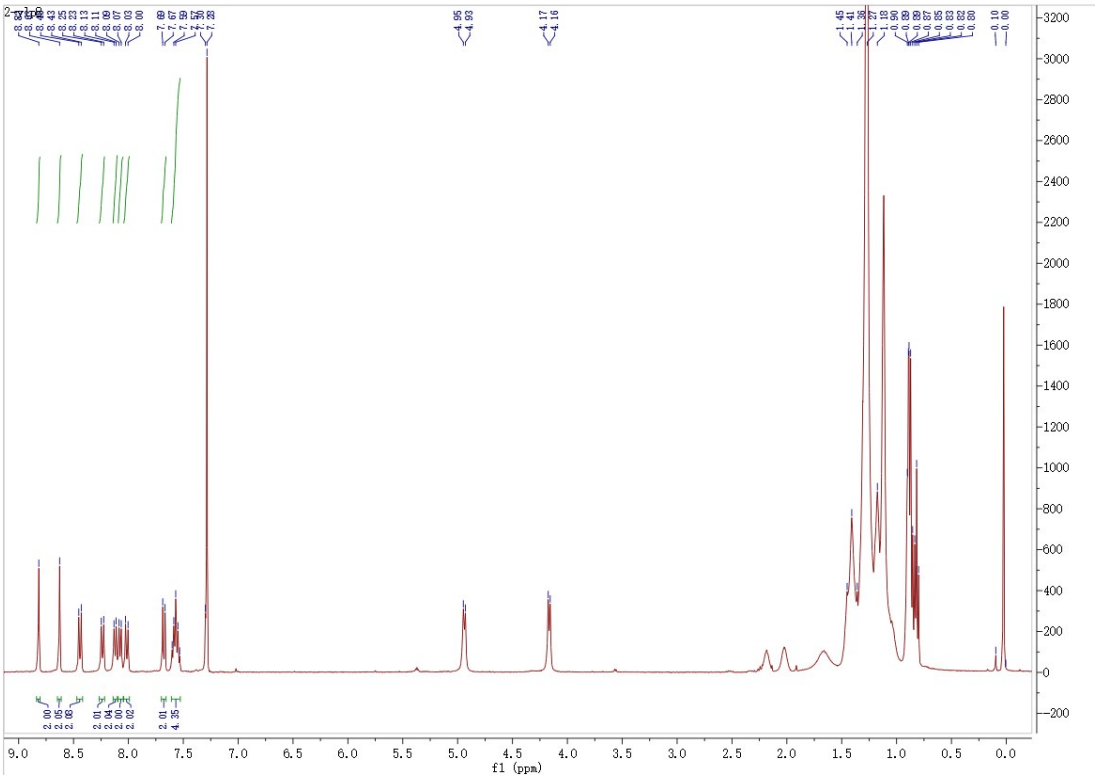

Figure S19:[1]H NMR of **AI-7** in $CDCl_3$ at 300K.

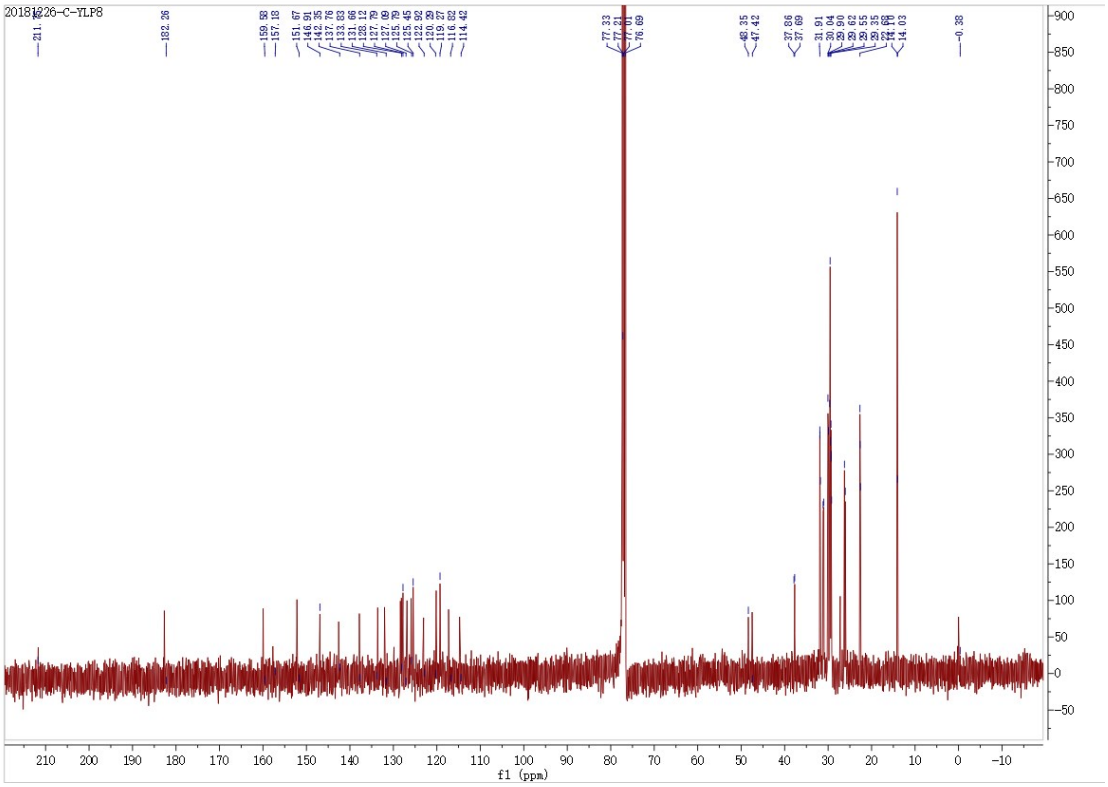

Figure S20 :[13]CNMR of **AI-7** in $CDCl_3$ at 300K.

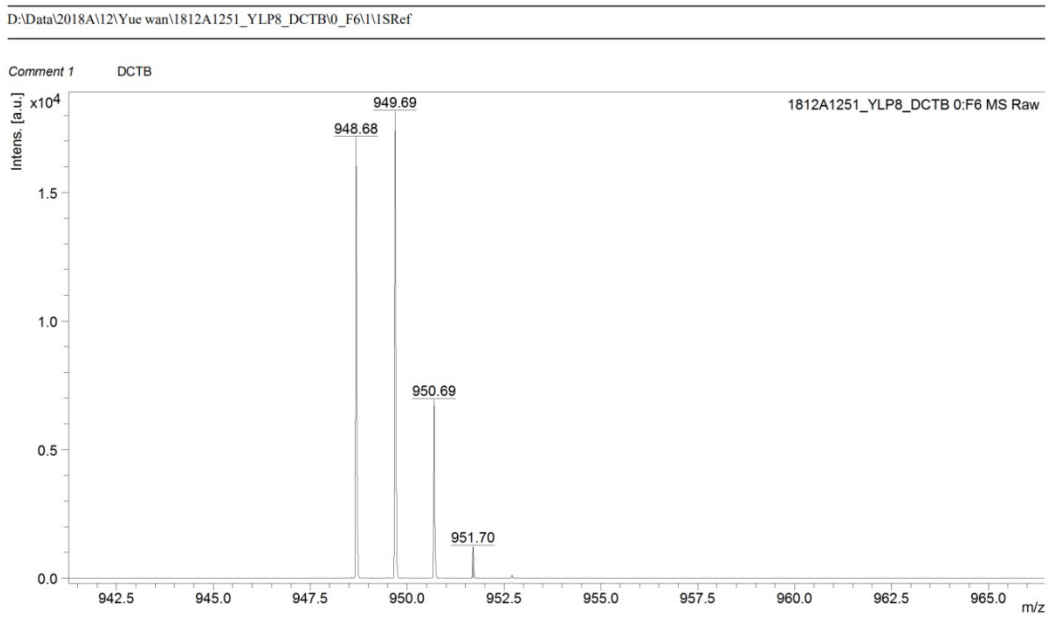

Figure S21: MALDI-TOF of **AI-7**.

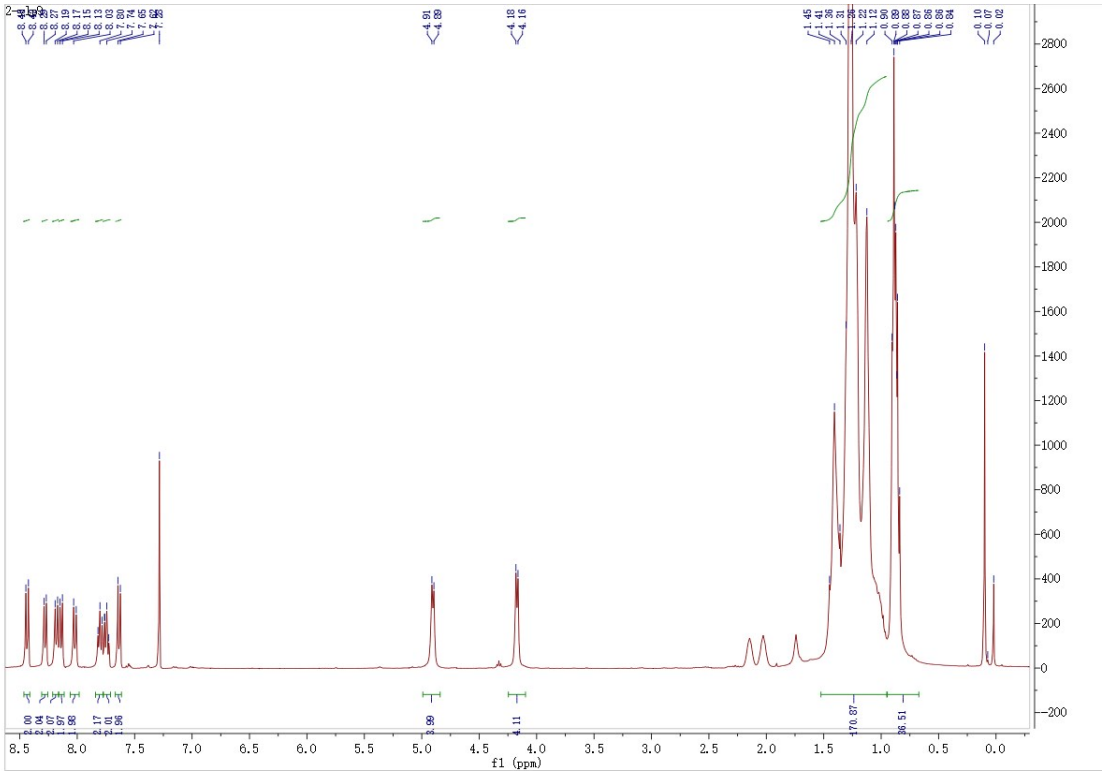

Figure S22: ^{1}H NMR of **AI-6** in $CDCl_3$ at 300K.

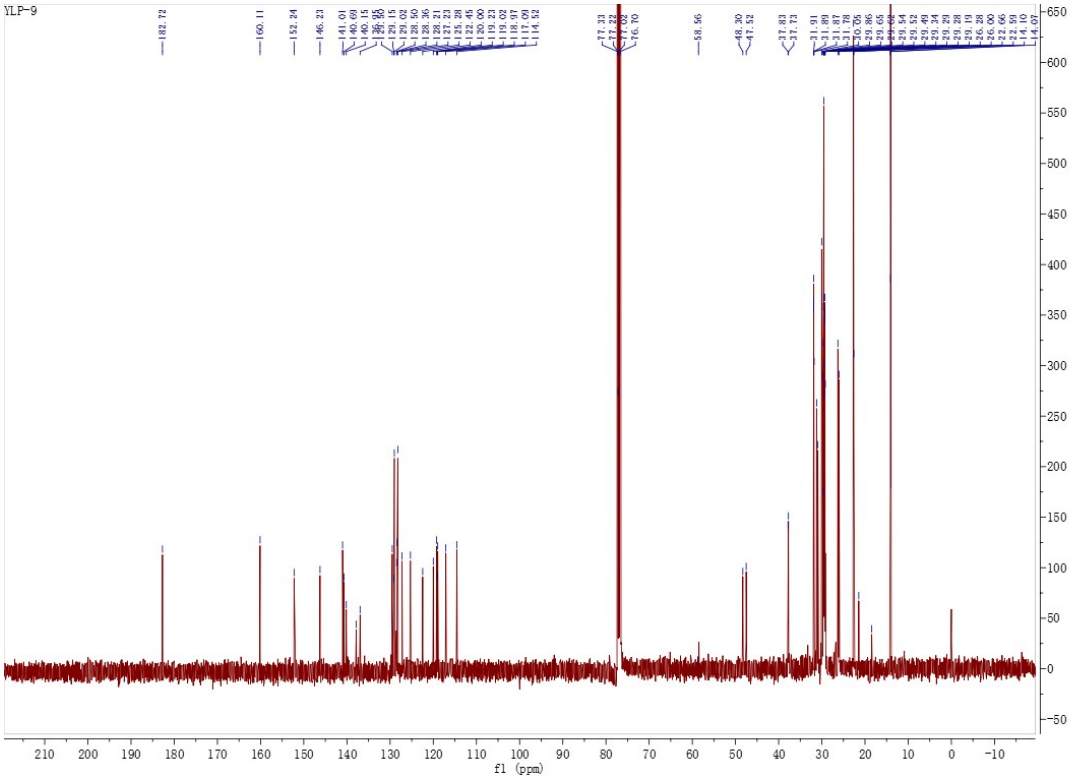

Figure S23:^{13}CNMR of **AI-6** in $CDCl_3$ at 300K.

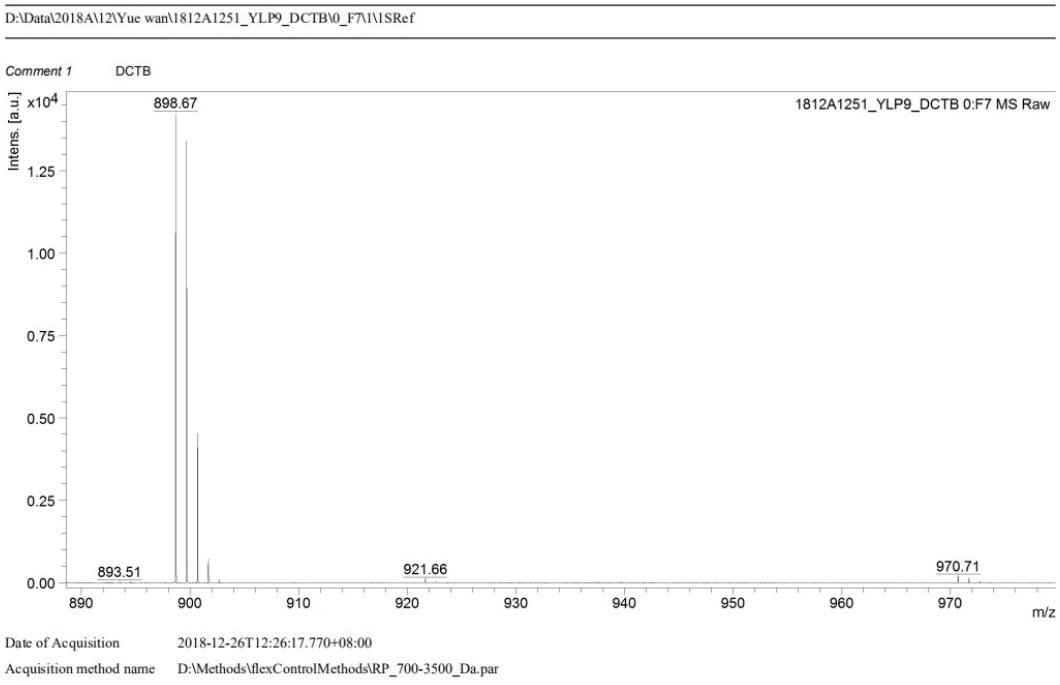

Figure S24: MALDI-TOF of **AI-6**.

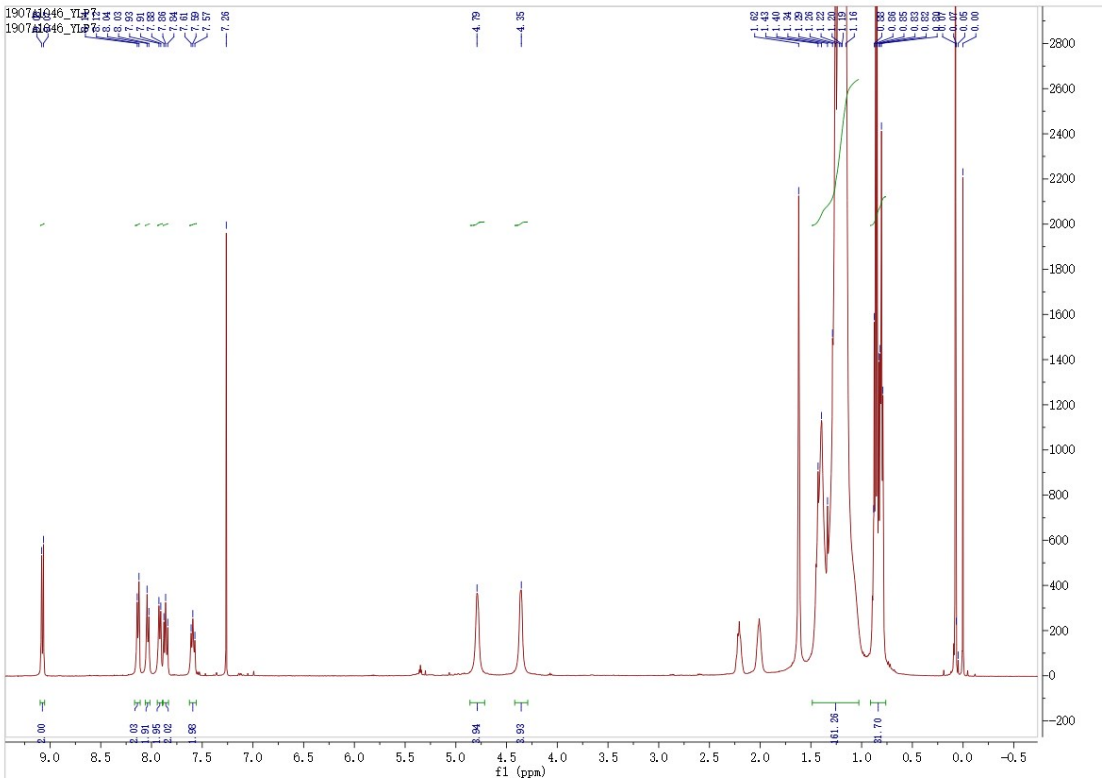

Figure S25: ^{1}H NMR of **FAIID-12** in $CDCl_3$ at 300K.

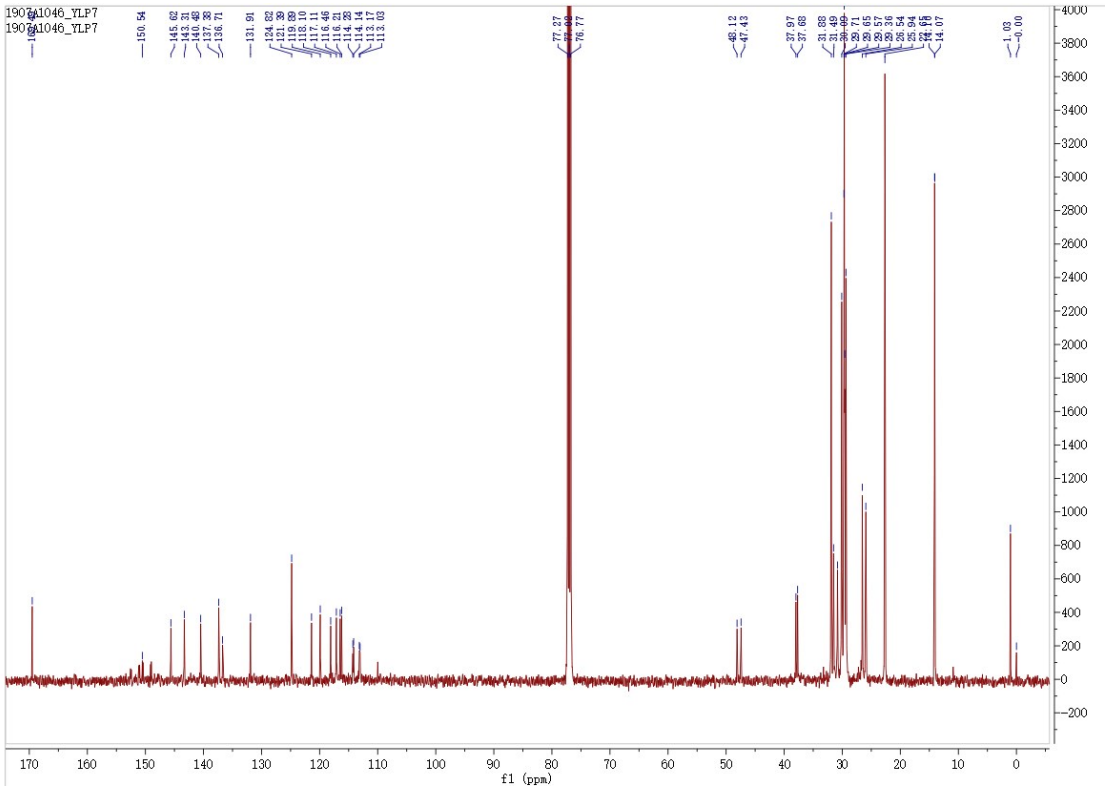

Figure S26:^{13}C NMR of **FAIID-12** in $CDCl_3$ at 300K.

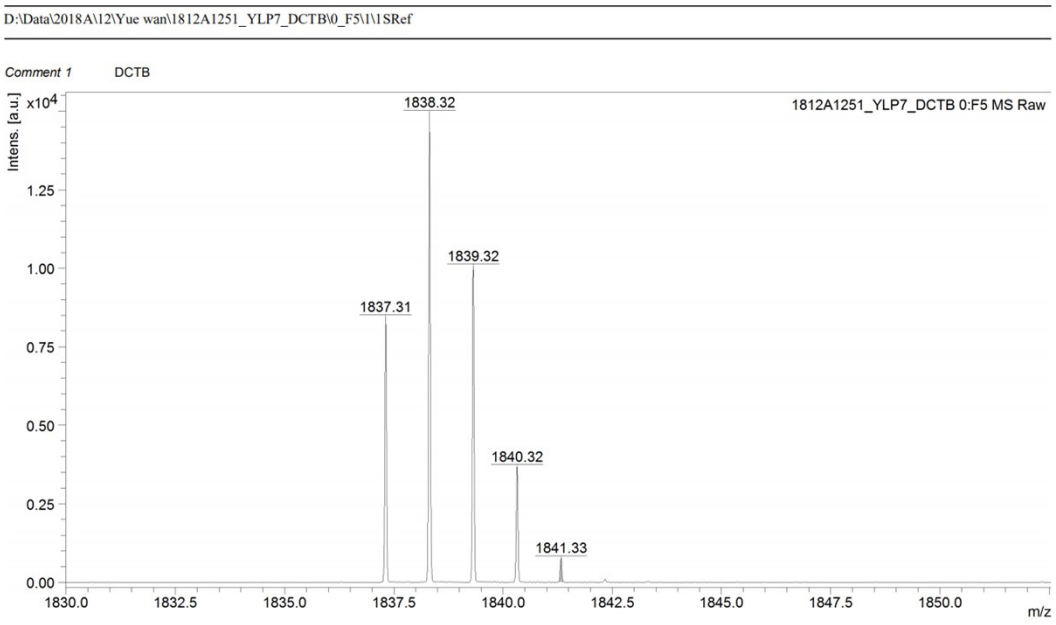

Figure S27: MALDI-TOF of **FAIID-12**.

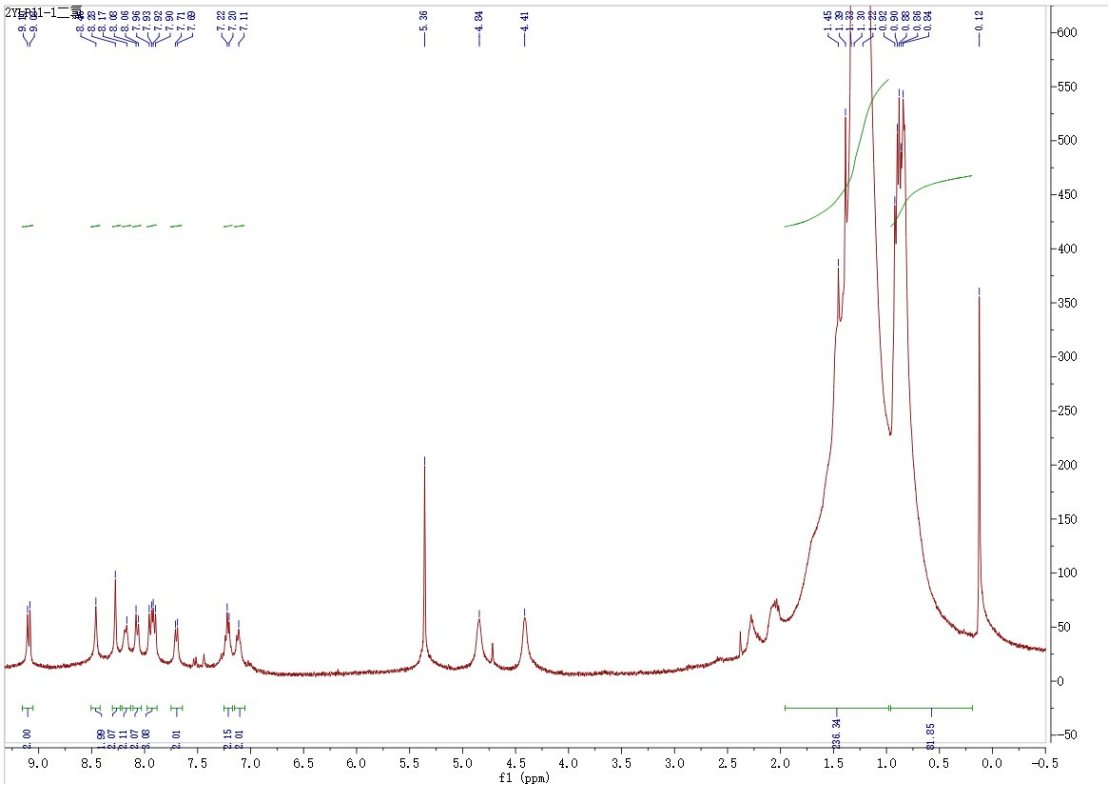

Figure S28: ^{1}H NMR of **AIID-14** in $CDCl_2$ at 300K.

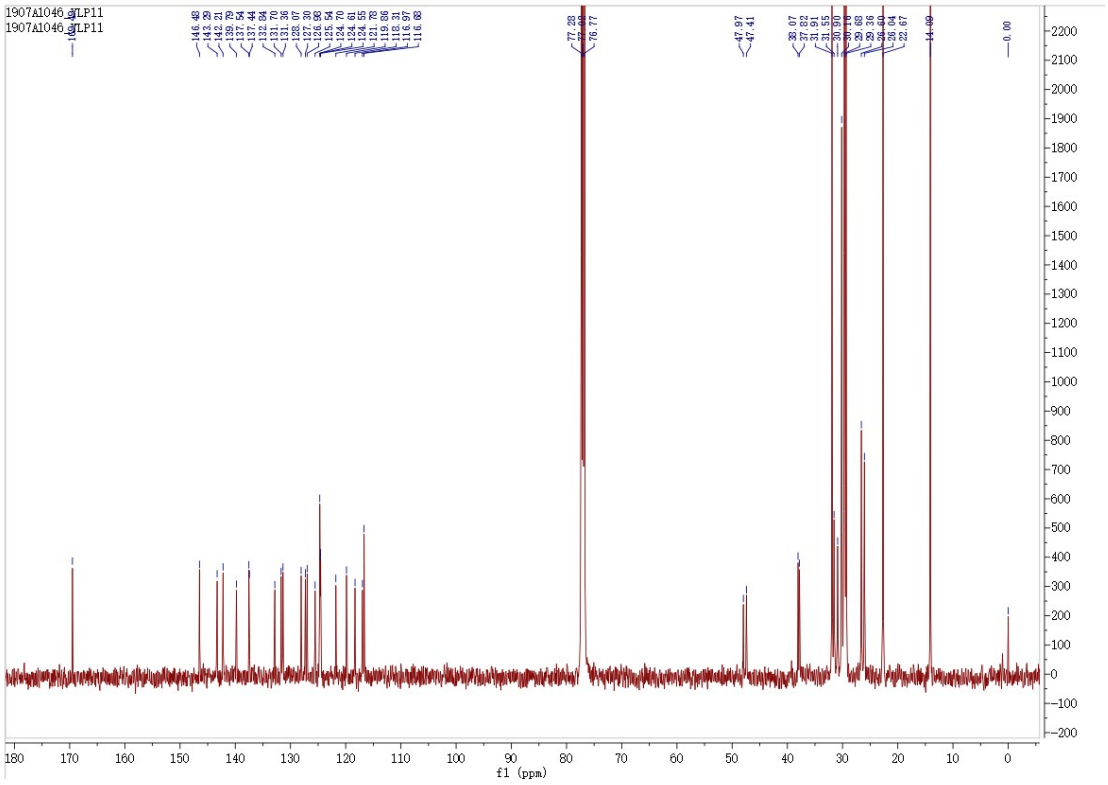

Figure S29:[13]CNMR of **AIID-14** in $CDCl_3$ at 300K.

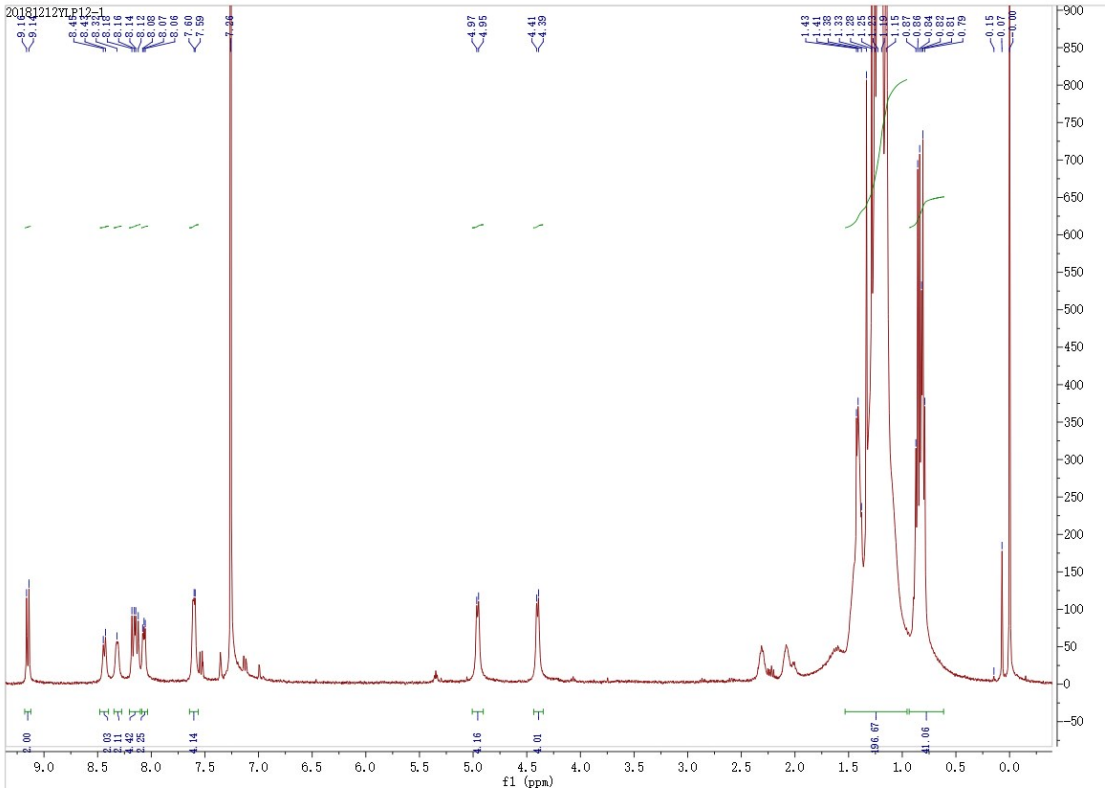

Figure S30: [1]H NMR of **AIID-12** in $CDCl_3$ at 300K.

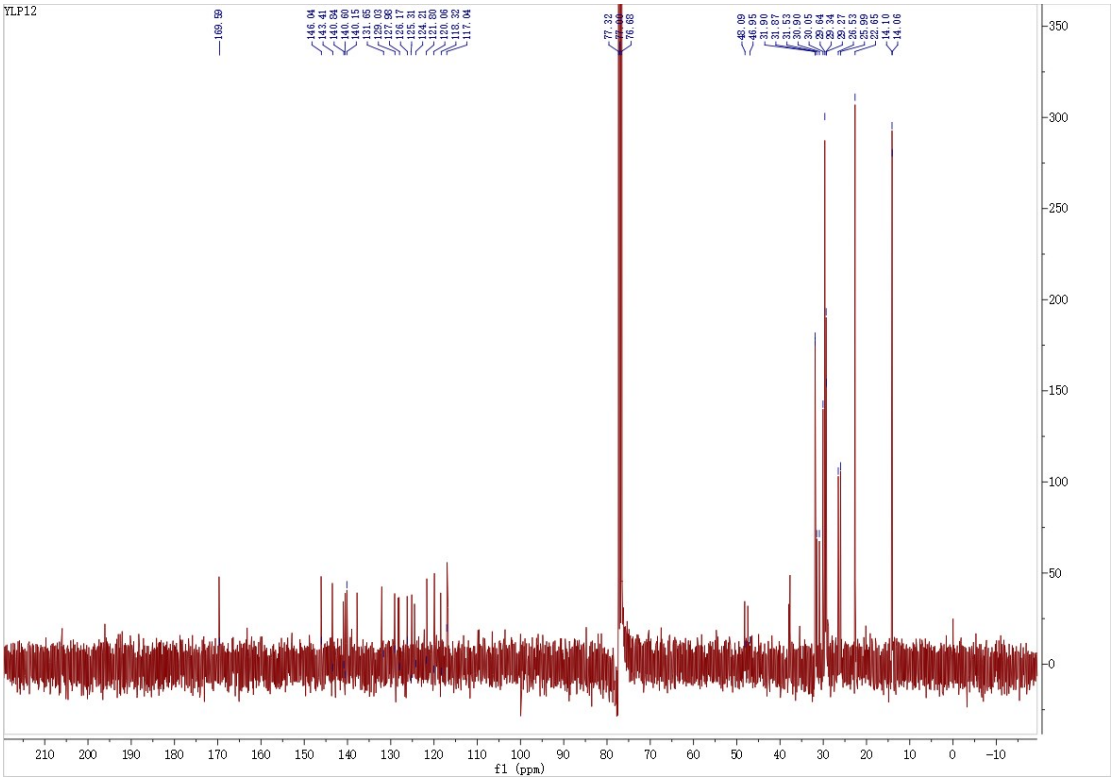

Figure S31:^{13}CNMR of **AIID-12** in $CDCl_3$ at 300K.

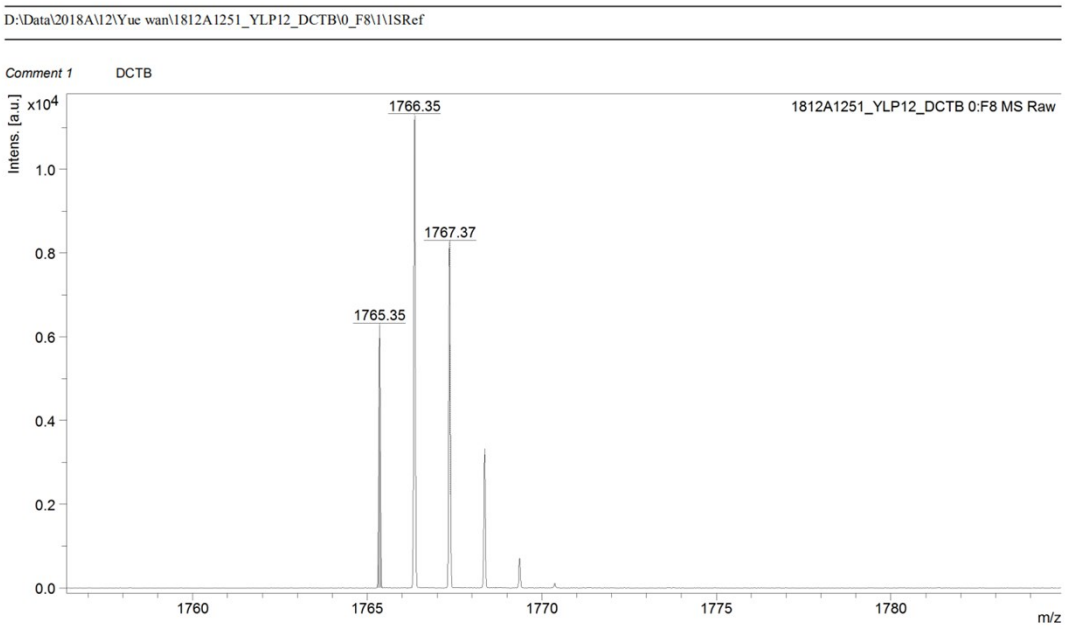

Figure S32: MALDI-TOF of **AIID-12**.

12. References

[1]: Gaussian 16, Revision C.01, Frisch, M. J.; Trucks, G. W.; Schlegel, H. B.; Scuseria, G. E.; Robb, M. A.; Cheeseman, J. R.; Scalmani, G.; Barone, V.; Petersson, G. A.; Nakatsuji, H.; Li,

X.; Caricato, M.; Marenich, A. V.; Bloino, J.; Janesko, B. G.; Gomperts, R.; Mennucci, B.; Hratchian, H. P.; Ortiz, J. V.; Izmaylov, A. F.; Sonnenberg, J. L.; Williams-Young, D.; Ding, F.; Lipparini, F.; Egidi, F.; Goings, J.; Peng, B.; Petrone, A.; Henderson, T.; Ranasinghe, D.; Zakrzewski, V. G.; Gao, J.; Rega, N.; Zheng, G.; Liang, W.; Hada, M.; Ehara, M.; Toyota, K.; Fukuda, R.; Hasegawa, J.; Ishida, M.; Nakajima, T.; Honda, Y.; Kitao, O.; Nakai, H.; Vreven, T.; Throssell, K.; Montgomery, J. A., Jr.; Peralta, J. E.; Ogliaro, F.; Bearpark, M. J.; Heyd, J. J.; Brothers, E. N.; Kudin, K. N.; Staroverov, V. N.; Keith, T. A.; Kobayashi, R.; Normand, J.; Raghavachari, K.; Rendell, A. P.; Burant, J. C.; Iyengar, S. S.; Tomasi, J.; Cossi, M.; Millam, J. M.; Klene, M.; Adamo, C.; Cammi, R.; Ochterski, J. W.; Martin, R. L.; Morokuma, K.; Farkas, O.; Foresman, J. B.; Fox, D. J. Gaussian, Inc., Wallingford CT, 2016.

[2] T. Lei, J -H. Dou, X-Y. Cao, J -Y. Wang, J. Pei, *J. Am. Chem. Soc*. 2013, 135, 12168−12171.